ACS APPLIED MATERIALS & INTERFACES

Research Article

www.acsami.org

Experimental Mixture Design as a Tool for the Synthesis of Antimicrobial Selective Molecularly Imprinted Monodisperse Microbeads

Elena Benito-Peña,[†] Fernando Navarro-Villoslada,[†] Sergio Carrasco,[†] Steffen Jockusch,[‡] M. Francesca Ottaviani,[§] and Maria C. Moreno-Bondi*[,†]

[†]Chemical Optosensors and Applied Photochemistry Group, Dept. of Analytical Chemistry, Faculty of Chemistry, Universidad Complutense, E-28040 Madrid, Spain

[‡]Department of Chemistry, Columbia University, New York, 3000 Broadway, New York, New York 10027, United States

[§]Department of Earth, Life and Environment Sciences (DiSTeVA), Loc. Crocicchia, I 61029 Urbino, Italy

Supporting Information

ABSTRACT: The effect of the cross-linker on the shape and size of molecular imprinted polymer (MIP) beads prepared by precipitation polymerization has been evaluated using a chemometric approach. Molecularly imprinted microspheres for the selective recognition of fluoroquinolone antimicrobials were prepared in a one-step precipitation polymerization procedure using enrofloxacin (ENR) as the template molecule, methacrylic acid as functional monomer, 2-hydroxyethyl methacrylate as hydrophilic comonomer, and acetonitrile as the porogen. The type and amount of cross-linker, namely ethylene glycol dimethacrylate, divinylbenzene or trimethylolpropane trimethacrylate, to obtain monodispersed MIP spherical beads in the micrometer range was optimized using a simplex lattice design. Particle size and morphology were assessed by scanning electron microscopy, dynamic light scattering, and nitrogen adsorption measurements. Electron paramagnetic resonance spectroscopy in conjunction with a nitroxide as spin probe revealed information about the microviscosity and polarity of the binding sites in imprinted and nonimprinted polymer beads.

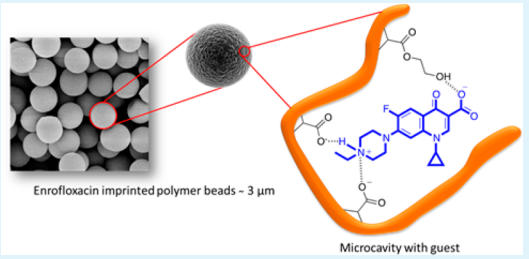

KEYWORDS: *molecular imprinting, precipitation polymerization, experimental design, microparticles, fluoroquinolones, EPR*

INTRODUCTION

Molecular imprinting is a template-directed polymerization technique that enables the synthesis of artificial selective molecular recognition materials. These polymers are usually regarded to as synthetic analogues of antibodies as they contain cavities that are complementary in size, shape, and functional group distribution to those of the template molecule present during polymerization.[1] To satisfy the different application purposes, molecularly imprinted polymers (MIPs) can be prepared in different formats, such as monoliths, beads, membranes, or nanostructures, among others.[2]

The preparation of bead-shaped MIPs, characterized by a narrow particle size distribution, is especially suited for analytical separations as these materials allow a more efficient packing of the chromatographic columns, or the solid phase extraction (SPE) cartridges, significantly improving the hydrodynamic properties of the system.[3−5] Moreover, the integrity of the binding sites is preserved after MIP synthesis as no further processing of the material is required for analytical application.[2] MIP beads have been applied as well in capillary electrophoresis,[6−8] fluorescent-based assays,[9] chemiluminescence imaging,[10] radioligand binding assays,[11] and sensors,[12] as well as for the preparation of composite membranes.[13]

There is a lack of a general procedure for the preparation of monodisperse spherical MIP beads, with different compositions and sizes in the micrometer range. Moreover, the need of strong interactions between the functional monomers and the template or the need of a high cross-linking degree to preserve the high-affinity binding sites limits the applicability of available synthetic methods for particle preparation.[14] Currently applied techniques include suspension polymerization, emulsion polymerization, dispersion/precipitation polymerization, single or multistep swelling polymerization, or surface imprinting on porous rigid supports in beaded form.[15] Probably, one of the most widely applied methods is precipitation polymerization. In this approach, polymerization takes place in a large excess of an organic solvent, where the monomers are soluble, but the resulting polymer is not, at monomer concentrations typically in the range of 2−5% (w/v).[16] In such conditions, polymer nuclei formed by aggregation of highly cross-linked oligomer radicals neither overlap nor coalesce but continue to grow individually by capturing new oligomers from solution

Received: March 13, 2015
Accepted: May 5, 2015
Published: May 5, 2015

DOI: 10.1021/acsami.5b02238
ACS Appl. Mater. Interfaces 2015, 7, 10966−10976

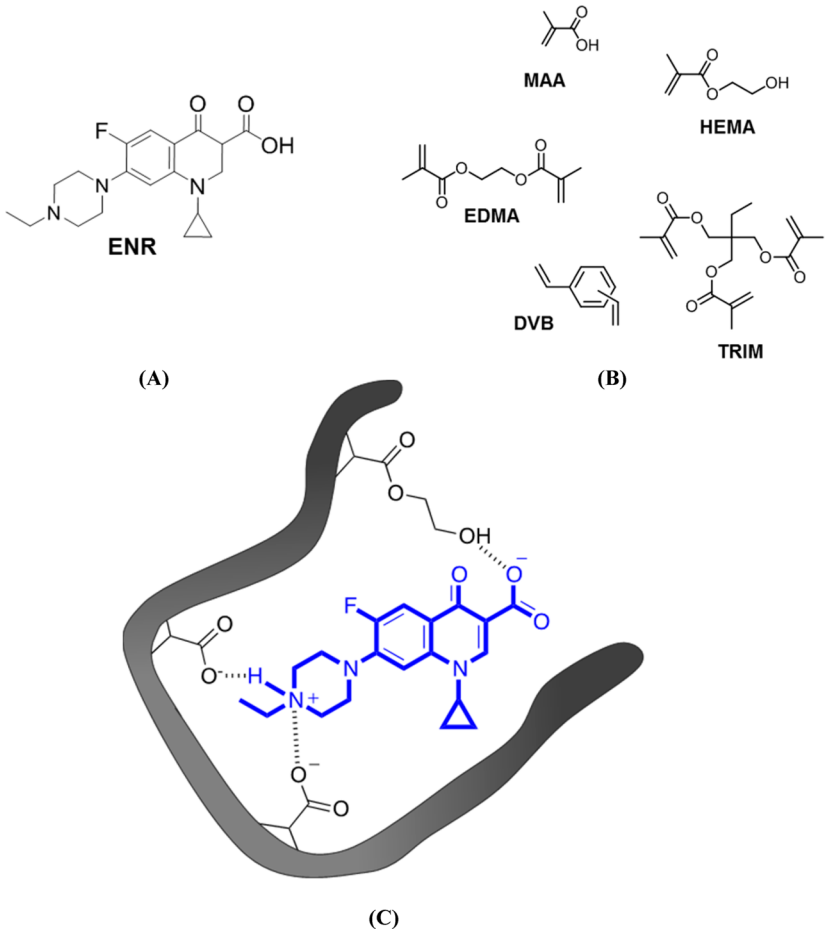

Figure 1. Structures of compounds used in this study (A) template molecule, (B) monomers and cross-linking monomers. (C) Schematic representation of ENR binding to a MIP selective cavity.

(entropic precipitation). In a reduced solvating medium, where the growing polymer has little affinity for the surrounding solvent, phase separation occurs, and nonporous polymer microspheres are obtained.

Several authors have studied the effect of the polymerization conditions on the size of particles obtained by this approach. Cormark, Sherrington, et al.[17,18] reported the preparation of MIP beads, with narrow size distributions and average diameter up to ca. 10 μm, using DVB as cross-linker, by adequately tuning the composition of the prepolymerization mixture (i.e., type of solvent and the monomers and initiator concentration). Mosbach and Ye described the use of a mixture of divinylbenzene (DVB) and trimethylolpropane trimethacrylate (TRIM) as cross-linkers, in different ratios, to prepare propranolol imprinted MIP beads with diameter sizes in the range 0.130−2.4 μm.[19] These authors pointed out the important influence of the presence of the template on the characteristics of the resulting beads, reporting that, for some compositions, the nonimprinted (NIP) particles were about 2 times larger than the corresponding MIPs. Other authors have described the preparation of monodisperse particles with sizes in the micrometer range (3−10 μm) for chromatographic applications.[17−22]

This study describes the preparation of micron-size monodisperse molecularly imprinted beads, with tunable sizes, by precipitation polymerization for their application in analytical separations. Enrofloxacin (ENR), a fluoroquinolone antimicrobial frequently used in veterinary medicine, was selected as a model template for polymer synthesis, although the main aim of the work was to study the effects of several parameters (e.g., the type and amount of porogenic solvent and the composition of the polymerization mixture) on the preparation of micrometer-size beads with a narrow size distribution. The polymers have been prepared using a combination of methacrylic acid (MAA) as functional monomer and 2-hydroxyethyl methacrylate (HEMA) as hydrophilic comonomer. An experimental mixture design (simplex lattice design) has been applied, for the first time, to study the effect of the type and amount of cross-linking monomer namely, ethylene glycol dimethacrylate (EDMA), DVB, or trimethylolpropane TRIM, on bead size and polydispersity (Figure 1). The texture and morphology of the functional surface of the MIPs have been investigated using scanning electron microscopy (SEM), transmission electron microscopy (TEM) and gas (N_2) adsorption. Electron paramagnetic resonance (EPR) spectroscopy was used to provide information on the differences in the binding cavities present in the imprinted and the corresponding nonimprinted polymers (NIP). Polymer cross-selectivity for other related and nonrelated antibiotics has been determined by HPLC.

EXPERIMENTAL SECTION

Chemicals. Methacrylic acid (MAA), 2-hydroxyethyl methacrylate (HEMA), divinylbenzene (DVB, technical grade, 55%, mixture of isomers), trimethylolpropane trimethacrylate (TRIM, technical grade) and ethylene glycol dimethacrylate (EDMA) were obtained from

DOI: 10.1021/acsami.5b02238
ACS Appl. Mater. Interfaces 2015, 7, 10966−10976

Sigma-Aldrich (St. Louis, MO). The monomers were purified using an inhibitor-remover from Aldrich (Milwaukee, WI). The initiator 2,2′-azobis(2,4-dimethylvaleronitrile) (ABDV) was purchased from Wako (Neuss, Germany), and it was recrystallized from methanol before use. Enrofloxacin (ENR) was supplied from Fluka (Buchs, Switzerland), and ciprofloxacin hydrochloride (CIP), norfloxacin (NOR), levofloxacin (LEV), flumequine (FLU), oxolinic acid (OXO), doxycycline (DOX), and nafcillin (NAF) were from Sigma-Aldrich (St. Louis, MO). Sarafloxacin hydrochloride (SAR) was a gift from Fort Dodge veterinaria (Girona, Spain) and danofloxacin (DAN) was obtained from Riedel-de-Haën (Seelze, Germany). Acetonitrile (ACN), methanol (MeOH) (HPLC-grade), and acetone (HPLC-grade) were provided by Sharlau Chemie (Barcelona, Spain), and trifluoroacetic acid (TFA) (HPLC-grade, 99%) was from Fluka (Buchs, Switzerland). Tetrahydrofuran (THF), dimethyl sulfoxide (DMSO) and *N*,*N*′-dimethylformamide (DMF) and 2-[4-(2-hydroxyethyl)-1-piperazinyl]-ethanesulfonic acid (HEPES) was supplied by Aldrich (Steinheim, Germany). The EPR probe, 4-(2′,2″,6′,6″-tetramethylpiperidine-1-*N*-oxyl)trimethylammonium bromide (CAT1) was synthesized following literature procedure.[23]

Water was purified using a Milli-Q system (Millipore, Bedford, MA). All solutions prepared for HPLC were passed through a 0.45 μm nylon filter before use.

Polymer Preparation. Molecularly imprinted micro- and nanoparticles were synthesized using precipitation polymerization. The template molecule, ENR (181.1 mg; 0.5 mmol) and the functional monomers, MAA (175 μL; 2 mmol) and HEMA (248 μL; 2 mmol), were dissolved in 15 mL of ACN in a 100 mL round-bottom flask. The cross-linkers DVB, EDMA, TRIM, or their mixtures, at the concentrations listed in Table 1, and the free radical initiator (ABDV, 1% weight of all monomers) were then added. The solution was homogenized and then purged with argon for 10 min. The solution was transferred to a borosilicate glass tube (50 mL) fit with a thermostated water jacket and the mixture was stirred (ca. 34 rpm) using a Heidolph RZR 2021 (Heidolph, Schwabach, Germany) mechanical overhead stirrer. The temperature was controlled with a digital water bath (Polyscience 9105 circulator, Polyscience, Niles, IL) and was held at 60 °C for 24 h. Upon completion of polymerization the particles were separated by centrifugation (Centrifuge 5804 R, Eppendorf, Stenvenage, UK) at 10 000 rpm for 10 min. For template removal, the particles were extracted by successive washing and centrifugation steps with methanol containing 5% TFA until no trace of the template was detected by chromatographic analysis of the washing solution with fluorescence detection. Finally, the particles were washed with a mixture of MeOH and acetone (1:1, v/v) and dried overnight in a vacuum oven at 40 °C. Non-imprinted (NIP) polymers were prepared in the same way as the MIPs but in the absence of the template molecule.

Table 1. Cross-Linker Composition in the Pre-Polymerization Mixture According to an Experimental Mixture Centroid Design

polymer	DVB (mmol)	TRIM (mmol)	EDMA (mmol)
MIP25	5	0	0
MIP26	0	0	5
MIP27	0	5	0
MIP28	2.5	0	2.5
MIP29	2.5	2.5	0
MIP30	0	2.5	2.5
MIP31	1.67	1.67	1.67

Polymer Characterization. Fourier Transform Infrared (FTIR) spectra of the polymers were obtained using a FTIR-8300 Shimadzu spectrophotometer (Shimadzu Corporation, Kyoto, Japan). Particle size and morphology were characterized by scanning electron microscopy (SEM) in a JEOL JSM-6400F Field Emission scanning electron microscope (JEOL Ltd., Tokyo, Japan) operating at 15 kV. Polymer samples were coated with gold before SEM measurements.

The particle-diameter dispersity (PDD) of the polymer microspheres was calculated from the SEM data measuring the size of, at least, 100 particles and applying the following equations:

$$\mathrm{PDD} = D_w/D_n \tag{1}$$

$$D_n = \sum_{i=1}^{k} n_i D_i / \sum_{i=1}^{k} n_i \tag{2}$$

$$D_w = \sum_{i=1}^{k} n_i D_i^4 / \sum_{i=1}^{k} n_i D_i^3 \tag{3}$$

where D_w the weight-average diameter, D_n is the number-average diameter, D_i the particle diameter of the beads, k the total number of measured particles and n_i the number of measured particles with the same diameter.[24,25]

Particle size distributions of the polymer microspheres were measured by dynamic light scattering using a CGS-8 (ALV GmbH, Hessen, Germany) instrument equipped with an Ar laser (Coherent I300, 514.5 nm). The average scattered intensity was recorded using a scattering angle of 30−140°, at 30 °C. The apparent hydrodynamic radius (R_H^{app}) of the particles was determined from the calculated apparent self-diffusion coefficient (D_{app}), by applying the Stokes−Einstein equation:[26]

$$D_{app} = \frac{k_B T}{6\pi\eta R_H^{app}} \tag{4}$$

where k_B is the Boltzmann constant, T is the temperature, and η is the solvent viscosity.

Porosity and surface area analysis were assessed by nitrogen adsorption−desorption porosimetry using an ASAP 2020 instrument (Micromeritics, Norcross, GA) at 77 K. Before the adsorption measurements, the samples were outgassed (10^{-3} Torr) at 50 °C for 2 h and at 30 °C for 8 h. The Brunauer−Emmett−Teller (BET) method was applied to calculate the specific surface area of the polymeric materials. The external surface area was obtained from the so-called t-plots calculated by the Harking and Jura equation while the pore size distribution was calculated by the Barret−Joyner−Halenda (BJH) method as described previously.[27]

Chromatographic Evaluation of Polymers. The polymers were packed into stainless columns (30 × 2.1 mm) using a slurry packer (Alltech Model 1666, Deerfield, IL) with methanol as packing solvent. Chromatographic analyses were carried out with an HP-1100 HPLC from Agilent Technologies (Palo Alto, CA) equipped with a quaternary pump, online degasser, autosampler, automatic injector, column thermostat, fluorescence detector and absorbance (diode array) detector. Fluoroquinolone stock solutions (200 μg mL^{-1}) were prepared in 0.02 M H_3PO_4 (0.01 M NaOH in the case of FLU and OXO). These solutions were stored at 4 °C in the dark for no longer than 1 month.

The binding affinity of the polymers to ENR (1 mM) was evaluated using different mobile phases ranging from 100% ACN to 100% HEPES buffer solution (0.1 M, pH 7.5). Analyses were performed at a flow of 0.2 mL min^{-1}, and the column temperature was kept at 25 °C. The injection volume was 20 μL and the UV detector was set to 260 nm. Cross-selectivity of the polymers toward structurally related analogues of the template molecule and other nonrelated compounds (Figure S1, SI) was evaluated under the same experimental conditions. The retention factor (k) for each analyte was calculated as $k = (t - t_0)/t_0$, where t and t_0 are the retention times of the analyte and the void marker (ACN containing 0.5% of acetone), respectively. Imprinting factors were evaluated as IF = k_{MIP}/k_{NIP}, where k_{MIP} and k_{NIP} are the retention factors of the analyte in the columns filled with MIP and NIP, respectively. Injections were carried out in triplicate.

The binding capacity of the polymers and the homogeneity of the binding sites were assessed by frontal chromatography following the procedure described by Kim and co-workers.[28] The MIP/NIP columns were equilibrated with ACN/water (0.1 M HEPES, pH 7.5) (50:50, *v*/*v*) as mobile phase. Solutions of the antimicrobials

DOI: 10.1021/acsami.5b02238
ACS Appl. Mater. Interfaces 2015, 7, 10966−10976

(0.03−0.50 mM), prepared in the mobile phase were pumped at a flow rate of 0.2 mL min^{-1} until a plateau in the fluorescence signal was attained. To ensure the complete removal of the analyte, we washed the columns after each measurement with 20 mL of methanol containing 0.5% of trifluoroacetic acid at 0.2 mL min^{-1} and re-equilibrated with 12 mL of the mobile phase before a new measurement. The breakthrough volume was calculated from the maximum numerical value of the first derivative of the frontal chromatogram. The breakthrough volume for a nonretained analyte was measured by eluting the columns with ACN containing 0.5% of acetone. All analyses were carried out in triplicate at room temperature.

The frontal analysis data were plotted in binding isotherms that were fitted to several isotherm adsorption models using SigmaPlot 11.0 (Systat Software Inc., San Jose, CA) for the calculation of the thermodynamic constants.

Hydrodynamic Performance of Polymer Particles. Pressure stability of the polymer was tested by packing the particles into a 20 × 2.1 mm stainless steel column (Upchurch Scientific, Oak Harbor, WA). The column was coupled to a HP-1100 quaternary pump (Agilent Technologies, Palo Alto, CA) and the pressure drop over the packed bed was measured at different flow rates of the mobile phase.[29]

The specific permeability was calculated according to Darcy's law (eq 5):

$$u = \frac{\Delta P K_0 d_p^2}{\eta L} \tag{5}$$

where u is the flow rate, ΔP is the column pressure drop, K_0 is the specific permeability, d_p is the average size of the particles, η is the viscosity of the solvent, and L is the length of the column. The system was run isocratically with ACN as mobile phase. ACN containing 0.5% acetone was used as the void marker. The pressure drop across the microparticle-size columns was monitored with the built-in pressure sensor of the pump. After the pressure test, the column was unpacked, and the particles were vacuum-dried before being subject to SEM.

Analysis by EPR. The polymers (2.5 mg) were incubated overnight in 1 mL of HEPES buffer (25 mM, pH 7.5) containing 0.5 mM CAT1. After centrifugation, the supernatant was removed, and the polymers were washed twice with the same buffer (1 + 1 mL) and transferred to capillary Pyrex tubes (1 mm inner diameter) for EPR measurements. UV spectroscopy was used to calculate the amount of CAT1 bound to the polymers by monitoring the absorbance of the supernatant solution, before and after incubation The retention of CAT1 in the MIP or NIP polymers was in the range of 1.2−1.7% (RSD < 5%, n = 3) for all the polymers tested. The EPR spectra were recorded on a Bruker EMX spectrometer operating at X-band (9.5 G) at room temperature. Computation of spectra was accomplished by utilizing the computer program developed by Freed, Budil, and co-workers.[30] The main parameters extracted from the spectral analysis are:

(1) The g_{ii} components of the g tensor for the coupling between the electron spin and the magnetic field. The values were g_{ii} = 2.009, 2.006, and 2.0023 and did not show significant variation between different samples, and therefore, they are not discussed further.

(2) The A_{ii} components of the coupling tensor between the electron spin and the nuclear nitrogen spin, A. For comparison, the average value $\langle A \rangle = (A_{xx} + A_{yy} + A_{zz})/3$, whose increase is related to an increase in environmental polarity of the radicals, is reported. The accuracy of this parameter is ±0.01 G.

(3) The correlation time for the rotational diffusion motion of the probe, τ. The Brownian diffusion model ($D_i = 1/(6\tau_i)$) was assumed in the computation, where D is the diffusion coefficient. In this case the main component of the correlation time for motion is the perpendicular component, τ. An increase in τ corresponds to a decrease in the radical mobility that, in turn, reflects the microviscosity and interactions of the radical with functional groups at the binding sites. The accuracy of this parameter is ±0.01 ns.

(4) The intrinsic line width (indicated as LW), which increases with the increase of spin−spin interactions arising from probes close to each other. The accuracy of this parameters is ±0.02 G.

In cases where the experimental spectra are constituted by two or three spectral components due to CAT1 in motionally different environments, the components were subtracted and computed separately to obtain the mobility and polarity parameters characteristic of each probe environment. The relative percentages of the probe populations were obtained from double integration of each spectral component. The accuracy of this parameters is ±1%.

Experimental Design and Data Processing. To evaluate the effect of the nature of the cross-linker on the size, dispersity, and yield of the polymer beads, we used an experimental mixture design in which factors represent the fraction of a given component in a mixture.[31,32] With the experimental results of the experimental design, a polynomial model, describing the relation between a response and the considered factors, was build.[33,34] The model was interpreted graphically, by drawing 2D contour plots, and statistically applying Analysis of Variance.

Three cross-linkers, namely, EDMA, DVB, and TRIM, have been considered as factors of interest, that is, ingredients of the mixture. The experimental mixture design used in this work was a simplex centroid design. In such approach, the experimentation points form a $\{q,n\}$ lattice in a (q-1) dimension simplex, where q is the number of components and n is the degree of the polynomial model. In a q-component simplex centroid design, the number of distinct points is 2^q-1. When q = 3 the constrained experimental region can be represented with an equilateral triangle as shown in Figure 2.

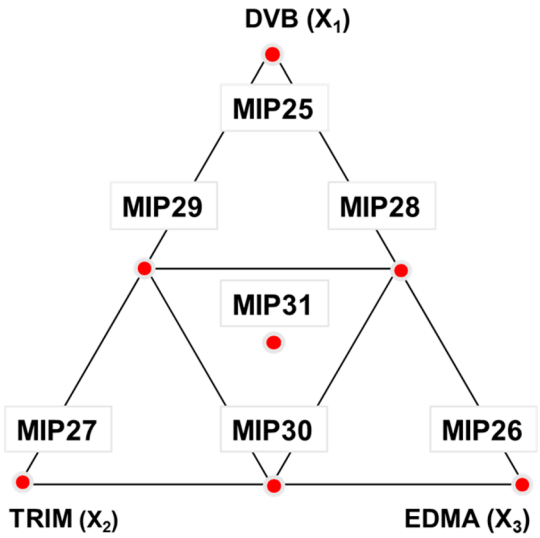

Figure 2. A three-component experimental mixture centroid design.

The coordinates of the seven designed points correspond to the amount of each cross-linker in the prepolymerization mixture. Thus, coordinates (1, 0, 0), (0, 1, 0), and (0, 0, 1) (vertices of the triangle) correspond to the pure q component (i.e., polymers synthesized with one cross-linker); coordinates (1/2, 1/2, 0), (0, 1/2, 1/2), and (1/2, 0, 1/2) (midpoints of the three sides of the triangle) are ascribed to binary mixtures (i.e., polymers synthesized mixing two cross-linkers) and the central point (1/3, 1/3, 1/3) (centroid) corresponds to the ternary mixture (i.e., a polymer synthesized mixing the three cross-linkers). Table 1 shows the cross-linker composition for the polymers synthesized in the experimental mixture design. The amount of template (ENR), functional monomers (MAA and HEMA), volume of ACN and percentage of initiator (ABDV) were kept constant throughout all the experiments.

After data were collected, they were fitted to a special cubic polynomial model applying least-squares regression to estimate the unknown coefficients in eq 6:

DOI: 10.1021/acsami.5b02238
ACS Appl. Mater. Interfaces 2015, 7, 10966−10976

$$Y = b_1X_1 + b_2X_2 + b_3X_3 + b_{12}X_1X_2 + b_{13}X_1X_3 + b_{23}X_2X_3 + b_{123}X_1X_2X_3 \quad (6)$$

where Y is the response, b_i is the magnitude of the effect of each component, b_{ij} is the magnitude of the synergistic or antagonistic effect of two-components, and b_{ijk} is the magnitude of the synergistic or antagonistic effect of the three components on the response. X_i denote the proportions of the q components in the mixture. The computer program Design-Expert 7.1.5 (Stat-Ease Inc., Minneapolis, MN) was used to analyze the results.

RESULTS AND DISCUSSION

In a previous study, we described the preparation of water-compatible ENR-imprinted polymers using bulk polymerization.[35] The polymers were synthesized using MAA as functional monomer, HEMA as hydrophilic comonomer, EDMA as cross-linker, and ACN as porogenic solvent. The MIP showed selective recognition to ENR and related structural analogues, allowing their direct extraction from aqueous samples. However, the irregular shape and particle size of the imprinted materials were a shortcoming for online SPE and μ-HPLC applications. In the present work, we have focused on the preparation of monodisperse ENR-selective MIP beads by precipitation polymerization with a controllable size in the range of 2−3 μm suitable for such applications. The same combination of functional monomers was selected as they provided selective recognition of the antimicrobials in aqueous rich samples. A number of factors including the nature and concentration of the polymerization components have been evaluated to determine their impact on the size and shape of the resulting MIPs.

Selection of Polymerization Solvent. Initially, we explored the effect of several porogenic solvents and solvent mixtures on the preparation of narrow disperse microparticles by precipitation polymerization. It has been shown that ACN is an effective solvent for the preparation of uniform polymeric beads using DVB as the cross-linker.[19] MIP particles with good capacities and porosities have also been described using mixtures of ACN and toluene (near θ-solvents) in combination with DVB, as the presence of the cosolvent improves the compatibility with the oligomers and retards phase separation during polymerization.[17,18] Therefore, we explored the ability of these solvents (V = 15 mL), as well as MeOH, THF, DMSO, or DMF, to promote microparticle formation in the polymerization of MIPs. The polymers were prepared by mixing ENR (0.5 mmol) as template, MAA (2 mmol) and HEMA (2 mmol) as functional monomers, and a mixture of DVB (2.5 mmol) and EDMA (2.5 mmol) as cross-linkers, in 15 mL solvent.

As reported by Goh and Stover, the Hansen solubility parameters have shown to be more useful than the Hildebrand parameter to explain the role of the solvent in the formation of micron sized particles in polymerizations involving MAA.[36] In agreement with these authors, decreasing the solvency of the medium favors polymer−polymer interactions thus promoting polymer desolvation and microspheres formation. Tables S1 and S2 (SI) summarize the three-dimensional Hansen solubility parameter values for the polymerization components and for the various solvents included in the study.

The Hansen's three-dimensional solubility parameters differentiate between three types of interactions between the polymer and the solvent (i.e., dispersive (δ_d), polar (δ_p), and hydrogen bonding (δ_h)). In this work, soluble MIP polymers were obtained when solvents with either low δ_p and δ_h (THF), or medium δ_p but high δ_h (MeOH) were used, while solvents with moderate δ_h (DMSO and DMF) led to coagulation. Neat ACN, with high δ_p (18 $MPa^{1/2}$) and low δ_h (6.1 $MPa^{1/2}$), led to the formation of narrow disperse microspheres with spherical shape and smooth surface, for both MIP and NIP.[37] The shapes and particle sizes of the MIP/NIP polymers prepared in the different solvents are summarized in Table S2 (SI).

To produce particles with higher porosities, we mixed a thermodynamically good solvent (toluene) with ACN to favor solvation of the incoming polymeric phase.[38] Li and Stover reported the effectiveness of such mixture for precipitation polymerizations when DVB was used as a cross-linker, as it yielded high-quality bead-shaped polymers with reasonable yields and well developed pore structure.[39] However, all our attempts to use toluene as cosolvent (ACN/toluene, 75:25 v/v) led to the formation of polydisperse nanoparticles when ENR was used as the template. We attribute this result to the low solvency of the ACN/toluene mixture toward the template and to the low solubility of the monomers, which do not match the Hansen solubility parameter for the solvent mixture and exert a negative effect on chain formation during the early stages of the precipitation polymerization process.

These results, together with the well-known performance of ACN in molecular imprinting polymerizations, led us to select ACN as porogen for the synthesis of the ENR imprinted beads.[40]

Effect of the Solvent Volume and Monomer Concentration. To investigate the effect of the porogen volume on the morphology and size of the resulting beads, we prepared several polymers, keeping constant the amount of template (ENR), functional monomers (MAA and HEMA) as well as cross-linker (EDMA) and increasing the volume of ACN (Table S3, SI). Figure S2 (SI) shows the SEM images of the beads prepared with increasing amounts of porogen. Higher solvent volumes led to a decrease in the particle size that ranged from 997 nm (MIP4) to 343 nm (MIP1) when the volume was increased from 15 to 40 mL, respectively. Volumes lower than 15 mL led to particle coagulation. It should also be mentioned that, according to the dynamic light scattering results, the apparent hydrodynamic radius (R_h) distribution of the polymer particles was extremely narrow (CV% < 7%; Figure S3, SI), reflecting the high quality shapes of the imprinted beads.

Increasing the amount of DVB resulted in spherical beads with larger average particle diameters, up to 2.9 μm. This suggests that higher amounts of DVB enhance the solubility of the oligomers leading to the formation of beads with larger particle diameter (Figure S4, SI). Similar results and morphologies have been reported for poly(MAA-*co*-DVB),[41] poly(MAA-*co*-PEGMM-*co*-EDMA),[36] and poly(DVB) microspheres,[39] where increasing the concentration of the cross-linking agent led to an increase in the particle size.

Effect of the Cross-Linking Monomer. *Type and Concentration.* The formation of stable spherical polymer particles by precipitation polymerization depends on both the type of cross-linker and its concentration in the prepolymerization mixture.[42] Thus, we evaluated the effect of both factors on the preparation of ENR selective MIP beads by applying a mixture design approach based on a simplex lattice design (Figure 2). The amount of template (ENR), functional monomers (MAA and HEMA), initiator (ABDV), and the volume of porogen (ACN) were kept constant, and the concentration of EDMA, DVB, TRIM, or a combination of the three was varied, as described in Table 1.

DOI: 10.1021/acsami.5b02238
ACS Appl. Mater. Interfaces 2015, 7, 10966−10976

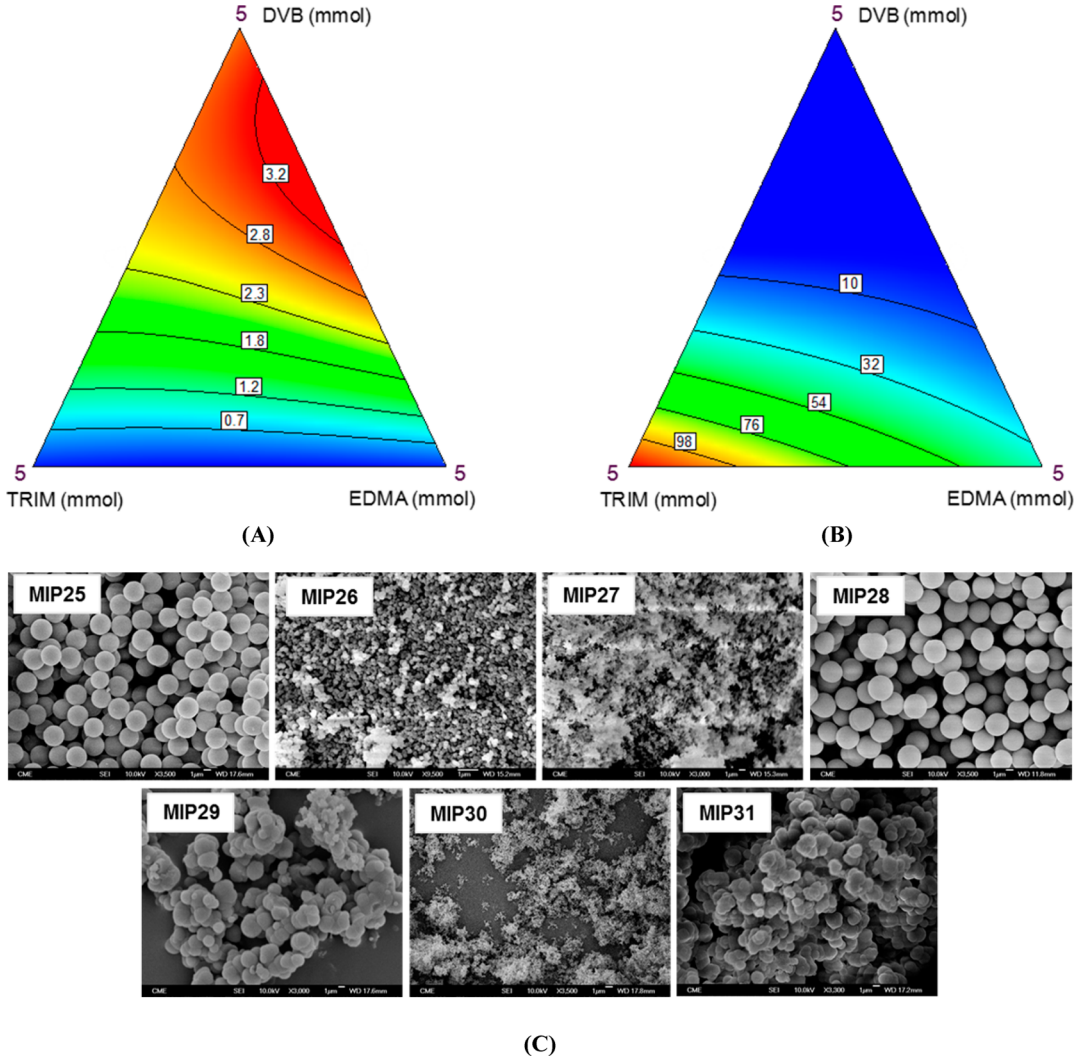

Figure 3. Response contour plots for the empirical models estimated by fitting (A) the average diameter and (B) the BET-specific surface area data of the MIPs as a function of the type and amount of cross-linker(s). (C) Scanning electron micrographs for the experimental mixture design formulations (see Table 1 and Figure 2).

Figure 3A,B shows the response contour plots for the fitted polynomial models obtained for the particle size and the surface area as a response, respectively. As shown in the SEM micrographs (Figure 3C), the MIPs showed important morphological differences, ranging from macrogels to microspheres, depending on the cross-linker(s) composition in the prepolymerization mixture. The use of DVB (MIP25) produced polymer beads with a narrow size distribution (2.86 ± 0.03 μm, PDD 1.00 ± 0.01) and low porosities (<5 m^2 g^{-1}). Besides, better shaped spherical particles (circularity close to 1) were obtained with increasing amounts of DVB in the prepolymerization mixture (Table 2). The polymers synthesized with EDMA (MIP26) or TRIM (MIP27) as cross-linkers were in the form of aggregates of particles or coagula with a high surface area (Figure 3). Polymer aggregates were also obtained when equimolar amounts of DVB/TRIM (molar ratio, 1:1) (MIP29) were used in the synthesis, with average particle sizes ranging between those obtained for DVB and TRIM-based MIPs. Moreover, the surface area of the DVB/TRIM polymer was similar to that of the one prepared with DVB, suggesting an important influence of this cross-linker on the porosity of the materials. The use of equimolar amounts of

Table 2. Average Diameter, BET Surface Area, and Circularity of the ENR Imprinted and the Corresponding Non-imprinted Polymer Microspheres

polymer[a]	diameter (μm)[b]	BET specific surface area (m^2 g^{-1})	circularity[c]
MIP25	2.86 ± 0.03	<5[d]	1.00 ± 0.01
NIP25	2.53 ± 0.01	<5[d]	1.00 ± 0.01
MIP26	0.21 ± 0.05	36.3 ± 0.4	0.89 ± 0.04
MIP27	0.19 ± 0.08	118 ± 1	0.6 ± 0.3
MIP28	3.22 ± 0.03	<5[d]	1.00 ± 0.01
NIP28	3.54 ± 0.06	<5[d]	1.00 ± 0.01
MIP29	2.4 ± 0.6	<5[d]	0.8 ± 0.1
MIP30	0.12 ± 0.02	82.8 ± 0.5	0.6 ± 0.1
MIP31	2.1 ± 0.3	17.0 ± 0.2	0.7 ± 0.1

[a]Polymer composition: template (ENR), 0.5 mmol (imprinted polymers); MAA, 2 mmol; HEMA, 2 mmol; cross-linker, see Table 1; initiator (ABDV), 1% (w/w); ACN, 15 mL. [b]Average diameter for at least 100 particles. [c]Circularity is defined as the ratio between the circumference of a circle of equivalent area to the particle and the perimeter of the particle itself. [d]Minimum surface area was determined with precision in the ASAP 2020 instrument (±confidence interval, α = 0.05).

DOI: 10.1021/acsami.5b02238
ACS Appl. Mater. Interfaces 2015, 7, 10966−10976

EDMA/DVB (molar ratio, 1:1) (MIP28) resulted in beads with a similar morphology to MIP25, but larger particle sizes (3.22 ± 0.03 μm, PDD 1.01 ± 0.01) and lower surface areas (<5 m^2 g^{-1}) were obtained with a higher yield (42%) than MIP25 (11%). However, bead circularity and surface roughness were very similar. Eventually, a mixture of the three cross-linkers (MIP31) resulted in a coagulum of microparticles with a 2.1 μm particle size and a surface area of 17 m^2 g^{-1}.

Interestingly, the particle size of NIP25, prepared with DVB (2.53 ± 0.01 μm) was slightly smaller than that of the corresponding MIP, but the opposite was observed when equimolar mixtures of DVB/EDMA were used (NIP28, 3.54 ± 0.06 μm), confirming that the presence of the template also exerts an important effect on the particle size.

To validate the empirical mixture model, we prepared a new MIP with a mixture of cross-linkers EDMA/DVB, at molar ratios of 1:4, which according to the empirical model should result in beads with a particle size of 3.4 ± 0.5 μm. The resulting polymer showed a similar morphology to MIP25 and MIP28 and a particle size of 2.89 ± 0.01 μm that does not significantly differ (α = 0.05) from the predicted value, confirming the adequate prediction ability of the empirical mixture model.

FTIR Analysis. The FTIR spectra of the imprinted polymers (Figure S5, Supporting Information) showed characteristic bands at ca. 1725 cm^{-1} (C═O stretch vibration), 3500 cm^{-1} (O−H stretch), 2950 cm^{-1} (C−H stretch), 1460 cm^{-1} (C−O−H bending), 1390 cm^{-1} (C−H bending) and 960 cm^{-1} (C−CH_3 bending). The polymers prepared with EDMA and TRIM showed the characteristic symmetric and asymmetric ester C═O stretching bands at 1260 and 1155 cm^{-1}, respectively.[43] However, these bands overlap when DVB was used as cross-linker (MIP28, MIP29). The spectra of the polymer prepared with DVB (MIP25) showed five bands at ca. 711, 798, 835, 903, and 990 cm^{-1} corresponding to the out-of-plane bending of the aromatic C−H.

The polymers prepared with cross-linker mixtures showed the characteristic IR bands for each monomer at relative intensity ratio that correlates with the polymerization ratios. In all cases, a band at ca. 1635 cm^{-1}, with moderate to weak intensity, assigned to the C═C stretch vibration was observed in the spectra reflecting the presence of unreacted double bonds.

EPR Analysis. EPR in conjunction with the positively charged nitroxide (CAT1) as probe was used to investigate the microenvironmental properties of the interior binding sites for ENR in MIP25 and MIP28 and compared to NIP25 and NIP28, respectively. EPR spectra were recorded after incubation of polymer particles in solutions containing CAT1 and washing (see Experimental Section). The EPR spectra were characteristic of two major components: CAT1 free in solution and CAT1 bound to the polymer particles. The free component was subtracted, and the bound component was subjected to computation. This bound component was, in turn, constituted by one or two components. The experimental and computed EPR spectra of CAT1 bound to polymer particles are shown in Figure 4, and the main parameters for computation are summarized in Table 3.

Significantly weaker EPR signals were observed for non-imprinted polymer particles compared to imprinted polymer particles, which is consistent with the lack of ENR binding sites for non-imprinted polymers. For example, the integrated signal intensity of the EPR spectrum for NIP25 was 5 times weaker than for MIP25 (Figure 4). The EPR spectrum of CAT1 bound to NIP25 was computed with a single component in slow motion conditions with a correlation time for the rotational mobility of τ = 5.37 ns. Two components were required to compute the spectrum of CAT1 bound to MIP25 and MIP28 (Table 3). The presence of two components for the MIPs indicates the presence of two binding sites in different environments, one more fluid and one less fluid (more viscous). The major component, at a relative percentage of 60% for MIP25 and 65% for MIP28, shows a lower mobility (τ = 5.6 ns). The minor component, 40% for MIP25 and 35% for MIP28, shows a faster mobility (τ = 2.35 ns). This minor component shows some line broadening (2 G) which might be caused by spin−spin interactions probably arising from a higher local concentration of CAT1 in MIPs.

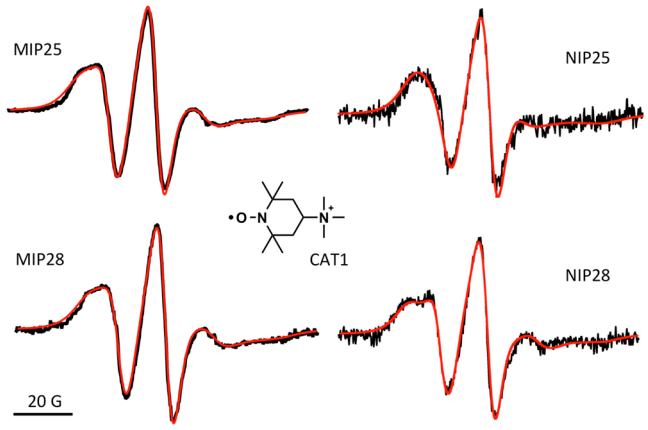

Figure 4. (Black) Experimental and (red) simulated EPR spectra of bound CAT1 on MIPs and NIPs.

Table 3. Main Parameters Extracted from the Computation of the EPR Spectra

sample	% component[a]	<A> (G)[b]	τ (ns)[c]	line width (G)[d]
MIP25	60	16.67	5.60	1.0
	40	16.67	2.35	2.0
NIP25	100	16.67	5.37	1.0
MIP28	65	16.70	5.60	1.0
	35	16.70	2.35	2.0
NIP28	70	16.83	6.30	0.7
	30	16.83	1.87	1.5
buffer[e]	100	16.78	0.05	0.7

[a]Percentage of signal contribution of the components (one or two) of bound CAT1 to MIPs and NIPs. [b]Average coupling constant. [c]Correlation time for rotational diffusion motion. [d]Intrinsic line width. [e]Free CAT1 in aqueous buffer solution.

Information on the polarity of the binding sites can be derived from the coupling constants ⟨A⟩ (Table 3). A higher ⟨A⟩ value corresponds to a higher polarity. The bound CAT1 showed a coupling constant of ⟨A⟩ = 16.67 G for MIP25 and NIP25 and ⟨A⟩ = 16.7 G for MIP28, which is slightly less polar than free CAT1 in aqueous solution (⟨A⟩ = 16.78 G). A slight increase in polarity of the binding site was observed for NIP28 (⟨A⟩ = 16.83 G). All investigated MIPs and NIPs showed relatively high coupling constants, which corresponds to polar binding sites. This is consistent with free carboxylic acid groups on the surface of the binding pockets.

Chromatographic Evaluation of the Polymer Microspheres. The binding capacity and selectivity of MIP25 and

DOI: 10.1021/acsami.5b02238
ACS Appl. Mater. Interfaces 2015, 7, 10966−10976

MIP28 to the antibiotic ENR were assessed by liquid chromatography. The beads were packed in a chromatographic column and the selective retention of FQ antimicrobials was evaluated using mixtures of ACN and 0.1 M HEPES buffer, pH 7.5 with increasing organic solvent content (0−100%, v/v) as mobile phase. As shown in Table 4, an imprinted effect is observed for ENR in pure ACN, both for MIP25 and MIP28. In fact, ENR was more strongly retained on MIP28 (no elution after 60 min) than on MIP25. The addition of 10% buffer decreases the retention times on both the MIP and the NIP, although the retention factor on the imprinted material remains always higher. The imprinting factor (IF) increases with the buffer concentration reaching a maximum at 75% aqueous buffer (IF ≥ 3.3) for both polymers. The retention times increased again at concentrations over 90% aqueous buffer; however, no selective retention was attained in such media, suggesting the presence of nonspecific hydrophobic interactions with the polymeric materials.

Table 4. Retention Behavior of ENR on MIP25/NIP25 and MIP28/NIP28 Polymers[a]

mobile phase ACN:HEPES buffer (0.1 M, pH 7.5)	k_{MIP25}[b]	k_{NIP25}[b]	IF[c]	k_{MIP28}[b]	k_{NIP28}[b]	IF[c]
100:0	77	16	4.8	NE[d]	NE[d]	
90:10	11	5.4	2.0	12	4.0	3.0
75:25	14	6.4	2.2	15	4.6	3.3
50:50	26	12	2.2	28	8.3	3.4
40:60	55	18	3.1	48	13	3.7
25:75	180	55	3.3	140	37	3.8
10:90	448	448	1.0	398	433	0.9
0:100	426	426	1.0	NE[d]	NE[d]	

[a]Analyte concentration, 1 mM; injection volume, 20 μL; flow rate, 0.2 mL min^{-1}. Column: 30 × 2.1 mm. [b]Retention factor calculated as $k = (t_r - t_0)/t_0$, where t_r is the retention time of the analyte, and t_0 is the retention time of an unretained component (void marker). [c]Imprinting factor: IF = k_{MIP}/k_{NIP}. (n = 3). [d]NE: not eluted after 60 min.

The binding properties and the homogeneity of the binding sites of MIP25 and MIP28 were assessed by frontal analysis. The binding features of ENR to both the MIPs and the NIPs were accurately modeled using the Freundlich isotherm model (Figure 5). The model developed by Rampey and co-workers (eq 7) was applied to estimate the affinity distribution, the apparent number of binding sites, $\bar{N}_{K_1-K_2}$, and the apparent weighted average affinity, $\bar{K}_{K_1-K_2}$, and the results are summarized in Table 5.[44]

$$N(K) = 2.303am(1 - m^2)e^{-2.303\log K} \quad (7)$$

The comparison of the affinity distributions of the polymers show that the binding capacity of MIPs is always higher than for the corresponding NIPs, especially for MIP25 (MIP25:6.9 ± 0.8 μmol g^{-1}; NIP25:1.8 ± 0.5 μmol g^{-1}; MIP28:4.7 ± 0.2 μmol g^{-1}; NIP28:1.1 ± 0.1 μmol g^{-1}). Slightly lower values of the heterogeneity index, meaning a more heterogeneous polymer, were obtained for MIP25 (0.62 ± 0.01), which also showed a higher average binding affinity (7558 ± 44 M^{-1}) for ENR than MIP28 (7283 ± 19 M^{-1}), as well as for the corresponding NIPs (NIP25:6499 ± 48 M^{-1}; NIP28:6440 ± 27 M^{-1}).

To evaluate the cross-selectivity of the imprinted microbeads and identify the noncovalent forces involved in the selective interaction of the polymers with a series of different antimicrobials, samples containing equimolar concentrations of the antibiotics (ENR, CIP, DAN, LEV, SAR, NOR, DOX, OXO, FLU) were injected in the MIP or NIP columns using different mobile phases (ACN/water (0.1 M HEPES, pH 7.5)). As can be observed in Figure 6, the highest IFs in both polymers were obtained with the template molecule (ENR); however, other structurally related fluoroquinolones, such as CIP, DAN, LEV, SAR, and NOR also showed good retention for buffer concentrations in the range from 25 to 75% (v/v) in the mobile phase (1.5 < IF < 2.2). As reported previously, selective retention can be explained considering the ionic interactions between the positively charged piperazinyl moiety on the antimicrobials and the carboxylate groups in the polymeric network.[35,45] Other fluoroquinolones such as OXO and FLU, which does not contain such ring, or other nonstructurally related antibiotics, DOX, showed IF < 1.2 in both polymers.

Application of MIP28 as a stationary phase for the separation of a solution of CIP, ENR, FLU, OXO, NAF, and DOX resulted in the chromatogram shown in Figure 7.

A solution of HEPES 50 mM containing 25% of ACN and 36 mM piperidine was selected as mobile phase. A pH gradient from pH 7.5 to 3.0 was applied to favor protonation of the

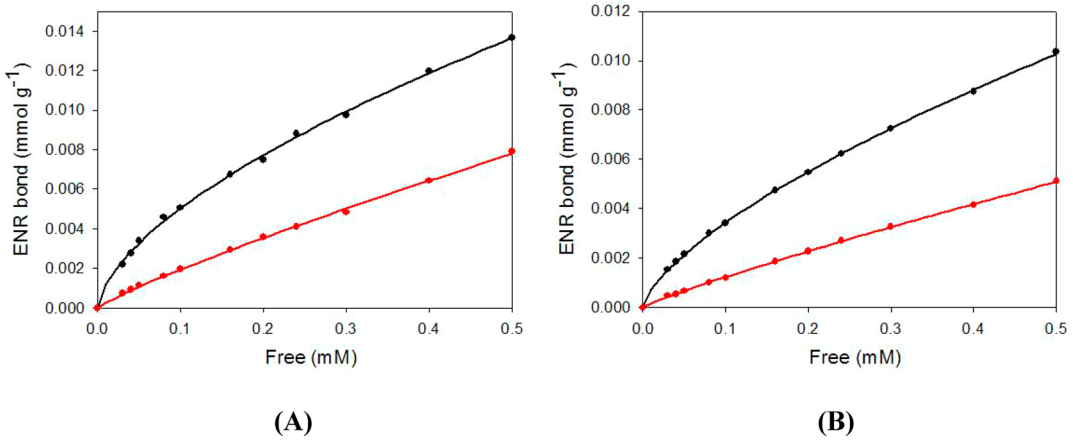

Figure 5. Adsorption isotherms of ENR on (black) MIPs and (red) NIPs for polymer (A) MIP25 and (B) MIP28 in ACN/HEPES buffer solution (0.1 M, pH 7.5) (50:50, v/v). Data fitted to a Freundlich adsorption isotherm model.

DOI: 10.1021/acsami.5b02238
ACS Appl. Mater. Interfaces 2015, 7, 10966−10976

Table 5. Freundlich Adsorption Isotherm Fitting Parameters, Apparent Weighted Average Affinity, and Apparent Number of Binding Sites[a,b]

	MIP25	NIP25	MIP28	NIP28
apparent weighted average affinity $\bar{K}_{K_1-K_2}$ $(M^{-1})^c$	7558 (44)	6499 (48)	7283 (19)	6440 (27)
apparent number of binding sites $\bar{N}_{K_1-K_2}$ $(\mu mol\ g^{-1})^c$	6.9 (0.8)	1.8 (0.5)	4.7 (0.2)	1.1 (0.1)
heterogeneity parameter n^d	0.62 (0.01)	0.86 (0.01)	0.68 (0.01)	0.88 (0.01)
preexponential factor, a $(\mu mol\ g^{-1}\ (L\ mol^{-1})^m)^d$	1531 (117)	5488 (538)	1798 (61)	4008 (219)
r^2	0.9988	0.9990	0.9998	0.9997

[a]Calculated according to ref 44. [b]Standard error in parentheses. [c]Free analyte concentration range, 0.03−0.5 mM (n = 3). [d]Freundlich adsorption isotherm model parameter. $B = aF^n$, where B and F are the concentrations of bound and free analytes, respectively.

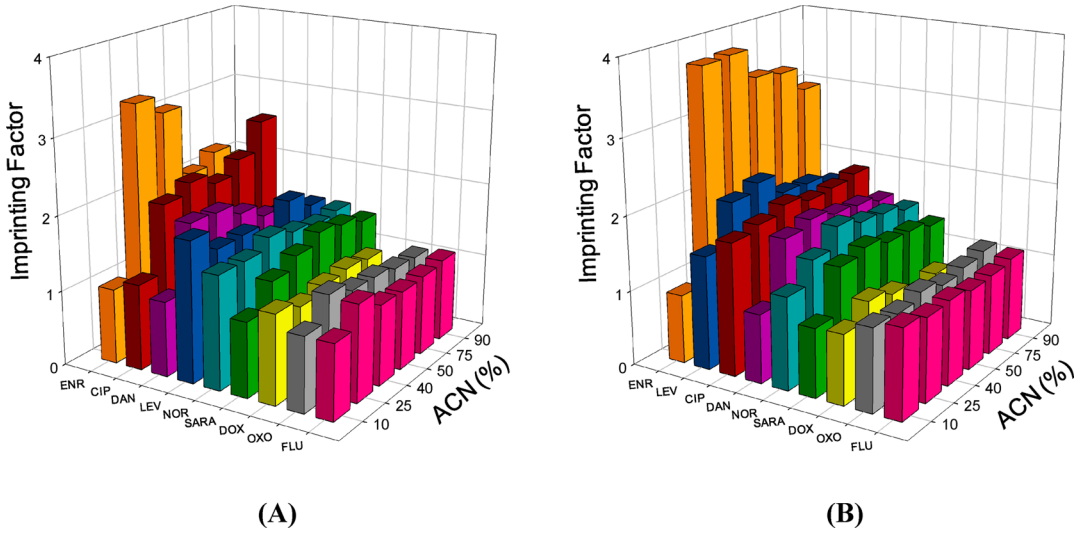

Figure 6. Cross-selectivity for ENR and structurally related and nonrelated analogs (see chemical structures in Figure S1, SI) in HPLC columns packed with (A) MIP25 and (B) MIP28. Solvent: ACN/HEPES buffer solution (0.1 M, pH 7.5). Imprinting factor (IF) calculated as IF = k_{MIP}/k_{NIP}. Retention factor (k) calculated as $k = (t_r - t_0)/t_0$, where t_r and t_0 are the retention time of the analyte and the void marker (acetone), respectively.

carboxyl groups in the MIP and, hence, facilitate the elution of the more retained analytes (Table S4, SI). The retention factors for CIP and ENR were 44 and 220, respectively. As expected from the cross-selectivity study, molecules lacking the piperazinyl moiety were poorly retained (k < 1.5) in the column. A baseline resolution (R_s = 1.6) between CIP and ENR confirmed the good performance of the MIP although a significant peak tailing was observed of both analytes that was attributed to the heterogeneity of the binding sites.

Polymer Stability and Compressibility. Packed MIP microspheres must withstand high pressures, without being compressed or collapse, to be useful for HPLC or "on-line" SPE applications. To evaluate the suitability of MIP25 and MIP28 in high-performance liquid chromatography, the polymers were packed in a 20 × 2.1 mm column and flowed with ACN as a mobile phase using a maximum packing pressure of 40 MPa.[31] MIP25 showed significantly higher backpressures than MIP28 at the same flow rates, probably due to a swelling effect. A plot of variation of the pressure drop vs the linear velocity of the mobile phase (Figure S6A, SI) showed a slight hysteresis for MIP25 and NIP25 polymers when they were subjected to a pressure drop up to 30 MPa. However, no hysteresis was observed for MIP28 and NIP28 in the same experimental conditions. A comparison of the SEM micrographs recorded before and after the test (Figure S7, SI) demonstrated that most MIP25 microbeads were cracked or dented upon pressure application; however, MIP28 beads showed no signs of compression or collapse.

The permeability of the MIP and NIP columns was evaluated using ACN as mobile phase (viscosity 0.37 cP at 25 °C).[46] The experimental data were fitted to Darcy's law (eq 5), as described in the Experimental Section, representing the specific permeability, considering the particles being nonporous, vs the linear velocity.[31] As shown in Figure S6B (SI) the specific permeability of MIP25 beads was significantly lower than for MIP28. This finding could be partially attributed to the different reactivity of both cross-linkers along with the clustering tendency of DVB that results in more compact and smaller particles with lower resistance to compressibility under high pressures. The non-imprinted polymers showed higher specific permeabilities than the corresponding MIPs, demonstrating that the cross-linker/template interactions during polymerization also affect the characteristics of the resulting polymers.[47]

CONCLUSIONS

An experimental mixture design strategy has been successfully applied to assess the influence of the cross-linker on the physicochemical characteristics of molecular imprinted microspheres selective to the antibiotic ENR prepared by precipitation polymerization. The application of a statistical mixture design has allowed unraveling the synergistic and antagonistic effects of different cross-linker blends on the morphology and porosity of MIPs, resulting in an optimal cross-linker composition to produce spherical MIP beads with suitable properties for analytical separations such as, micro-

DOI: 10.1021/acsami.5b02238
ACS Appl. Mater. Interfaces 2015, 7, 10966−10976

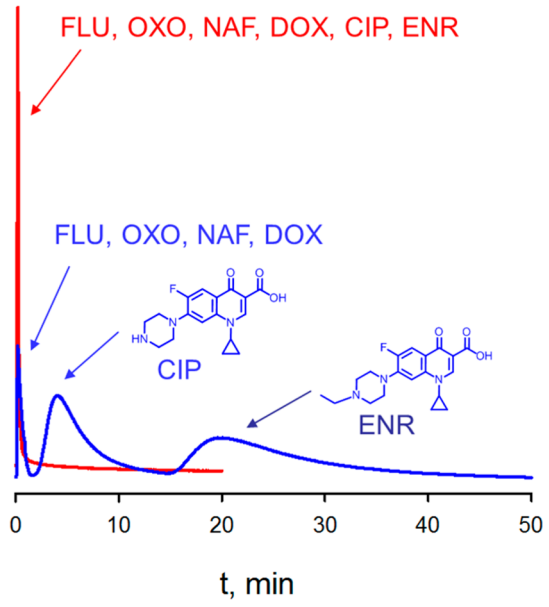

Figure 7. Elution profile of enrofloxacin (ENR), ciprofloxacin (CIP), flumequine (FLU), oxolinic acid (OXO), and nafcillin (NAF) using (blue) MIP28 and (red) NIP28 as stationary phases in HPLC. Column dimensions, 30 × 2.1 mm; mobile phase, ACN/HEPES buffer solution (50 mM) 50:50 (v/v) containing piperidine as modifier; pH gradient, 7.5−3 with 0.1% TFA in ACN; flow rate, 0.5 mL min^{-1}; detection, 280 nm; injection volume, 20 μL; analyte concentration, 1 mM.

meter particle size, narrow size distribution, low porosity, high hardness.

■ ASSOCIATED CONTENT

Supporting Information

Chemical structures of antimicrobials used in this study; estimated Hansen solubility parameters; morphology of MIPs synthesized in different solvents; particle diameter distribution and SEM images of MIPs obtained with different volume of acetonitrile; apparent hydrodynamic radio variation with the volume of acetonitrile. Particle-diameter dispersity and particle size of MIP particles as a function of the amount of DVB; FTIR spectra of MIPs; chromatographic method optimization; and pressure drop and specific permeability for selected polymers. The Supporting Information is available free of charge on the ACS Publications website at DOI: 10.1021/acsami.5b02238.

■ AUTHOR INFORMATION

Corresponding Author

*E-mail: mcmbondi@ucm.es. Phone: 0034-91394-5147. Fax: 0034-91394-4329.

Funding

The authors gratefully acknowledge financial support from MINECO (CTQ2012−37573-C02−02). S.J. thanks the National Science Foundation USA for financial support (CHE 1111392).

Notes

The authors declare no competing financial interest.

■ ACKNOWLEDGMENTS

S.C. and M.C.M.B. thank the Spanish Ministry of Education, Culture and Sport for a doctoral grant (FPU) and a grant for her sabbatical leave, respectively. The authors thank Prof. M. J. Torralvo for the N_2 adsorption studies. This work is dedicated to the memory of Prof. Turro.

■ REFERENCES

(1) *Molecular Imprinting*; Haupt, K., Ed.; Springer: Heidelberg, 2012.
(2) Biffis, A.; Drakova, D.; Falcimaigne-Cordin, A. Physical Forms of MIPs. *Top. Curr. Chem.* **2012**, *325*, 29−82.
(3) Lei, Y.; Cormack, P. A. G.; Mosbach, K. Molecular Imprinting on Microgel Spheres. *Anal. Chim. Acta* **2001**, *435*, 187−196.
(4) Ansell, R. J. Molecularly Imprinted Polymers in Pseudoimmunoassay. *J. Chromatogr. B* **2004**, *804*, 151−165.
(5) Haginaka, J. Monodispersed, Molecularly Imprinted Polymers as Affinity-Based Chromatography Media. *J. Chromatogr. B* **2008**, *866*, 3−13.
(6) de Boer, T.; Mol, R.; de Zeeuw, R. A.; de Jong, G. J.; Sherrington, D. C.; Cormack, P. A. G.; Ensing, K. Spherical Molecularly Imprinted Polymer Particles: A Promising Tool for Molecular Recognition in Capillary Electrokinetic Separations. *Electrophoresis* **2002**, *23*, 1296−1300.
(7) Schweitz, L.; Spegel, P.; Nilsson, S. Molecularly Imprinted Microparticles for Capillary Electrochromatographic Enantiomer Separation of Propranolol. *Analyst* **2000**, *125*, 1899−1901.
(8) Spegel, P.; Schweitz, P.; Nilsson, S. Selectivity Toward Multiple Predetermined Targets in Nanoparticle Capillary Electrochromatography. *Anal. Chem.* **2003**, *75*, 6608−6613.
(9) Hunt, C. E.; Pasetto, P.; Ansell, R. J.; Haupt, K. A Fluorescence Polarisation Molecular Imprint Sorbent Assay for 2,4-D: A Non-Separation Pseudo-Immunoassay. *Chem. Commun.* **2006**, *16*, 1754−1760.
(10) Wang, L.; Zhang, Z. Chemiluminescence Imaging Assay Dipyridamole Based on Molecular Imprinted Polymer as Recognition Material. *Sens. Actuators, B* **2008**, *133*, 40−45.
(11) Tse Sum Bui, B.; Belmont, A. S.; Witters, H.; Haupt, H. Molecular Recognition of Endocrine Disruptors by Synthetic and Natural 17β-estradiol Receptors: A Comparative Study. *Anal. Bioanal. Chem.* **2008**, *390*, 2081−2088.
(12) Suriyanarayanan, S.; Cywinski, P. J.; Moro, A. J.; Mohr, G. J.; Kutner, W. Chemosensors Based on Molecularly Imprinted Polymers. *Top. Curr. Chem.* **2012**, *325*, 165−265.
(13) Silvestri, D.; Borrelli, C.; Giusti, P.; Cristallini, C.; Ciardelli, G. Polymeric Devices Containing Imprinted Nanospheres: A Novel Approach to Improve Recognition in Water For Clinical Uses. *Anal. Chim. Acta* **2005**, *542*, 3−13.
(14) Pérez-Moral, N.; Mayes, A. G. In *Molecular Imprinting of Polymers*; Piletsky, S., Turner, A., Eds.; Landes Bioscience: Georgetown, 2006; Chapter 1, pp 1−11.
(15) Ye, L.; Yilmaz, E. In *Molecularly Imprinted Materials. Science and Technology*; Yan, M., Ramström, O., Eds.; Marcel Dekker: New York, 2005; Chapter 17, pp 435−454.
(16) Ramstrom, O.; Ye, L.; Krook, M.; Mosbach, K. Screening of a Combinatorial Steroid Library Using Molecularly Imprinted Polymers. *Anal. Commun.* **1998**, *35*, 9−11.
(17) Wang, J.; Cormack, P. A. G.; Sherrington, D. C.; Khoshdel, F. Synthesis and Characterization of Micrometer-Sized Molecularly Imprinted Spherical Polymer Particulates Prepared via Precipitation Polymerization. *Pure Appl. Chem.* **2003**, *79*, 1505−1519.
(18) Wang, J.; Cormack, P. A. G.; Sherrington, D. C.; Khoshdel, F. Monodisperse, Molecularly Imprinted Polymer Microspheres Prepared by Precipitation Polymerization for Affinity Separation Applications. *Angew. Chem., Int. Ed.* **2003**, *42*, 5336−5338.
(19) Yoshimatsu, K.; Reimhult, K.; Krozer, A.; Mosbach, K.; Sode, K.; Ye, L. Uniform Molecularly Imprinted Microspheres and Nanoparticles Prepared by Precipitation Polymerization: The Control of Particle Size Suitable for Different Analytical Applications. *Anal. Chim. Acta* **2007**, *584*, 112−121.
(20) Lai, J. P.; Yang, M. L.; Niessner, R.; Knopp, D. Molecularly Imprinted Microspheres and Nanospheres for Di(2-ethylhexyl)-phthalate Prepared by Precipitation Polymerization. *Anal. Bioanal. Chem.* **2007**, *389*, 405−412.

DOI: 10.1021/acsami.5b02238
ACS Appl. Mater. Interfaces 2015, 7, 10966−10976

(21) Jin, Y.; Jiang, M.; Shi, Y.; Lin, Y.; Peng, Y.; Dai, V.; Lu, B. Narrowly Dispersed Molecularly Imprinted Microspheres Prepared by a Modified Precipitation Polymerization Method. *Anal. Chim. Acta* **2008**, *612*, 105−116.
(22) Fontanals, N.; Marcé, R. M.; Cormack, P. A. G.; Sherrington, D. C.; Borrull, F. Monodisperse, Hypercrosslinked Polymer Microspheres as Tailor-Made Sorbents for Highly Efficient Solid-Phase Extractions of Polar Pollutants from Water Samples. *J. Chromatogr. A* **2008**, *1191*, 118−124.
(23) Kwan, C. L.; Atik, S.; Singer, L. A. An Electron Spin Resonance Study of the Association of a Surfactant Nitroxyl Radical With a Cationic Micelle Using Spin-Intensity Measurements and Hyperfine Structure Analyses. *J. Am. Chem. Soc.* **1987**, *100*, 4783−4786.
(24) Gilbert, R. G.; Hess, M.; Jenkins, A. D.; Jones, R. G.; Kratochvil, P.; Stepto, R. F. T. Dispersity in Polymer Science. *Pure Appl. Chem.* **2009**, *81*, 351−353.
(25) Carbajo, M. C.; Climent, E.; Enciso, E.; Torralvo, M. J. Characterization of Latex Particle Arrays by Gas Adsorption. *J. Colloid Interface Sci.* **2005**, *284*, 639−645.
(26) *Light Scattering from Polymer Solutions and Nanoparticle Dispersions*; Schärtl, W., Ed.; Springer-Verlag: Berlin, 2007.
(27) Urraca, J. L.; Carbajo, M. C.; Torralvo, M. J.; González-Vázquez, J.; Orellana, G.; Moreno-Bondi, M. C. Effect of the Template and Functional Monomer on the Textural Properties of Molecularly Imprinted Polymers. *Biosens. Bioelectron.* **2008**, *24*, 155−161.
(28) Kim, H.; Kaczmarski, K.; Guiochon, G. Mass Transfer Kinetics on the Heterogeneous Binding Sites of Molecularly Imprinted Polymers. *Chem. Eng. Sci.* **2005**, *60*, 5425−5435.
(29) Limé, F.; Irgum, K. Preparation of Divinylbenzene and Divinylbenzene-*co*-glycidyl Methacrylate Particles by Photoinitiated Precipitation Polymerization in Different Solvent Mixtures. *Macromolecules* **2009**, *42*, 4436−4440.
(30) Budil, D. E.; Lee, S.; Saxena, S.; Freed, J. H. Nonlinear-Least-Squares Analysis of Slow-Motion EPR Spectra in One and Two Dimensions Using a Modified Levenberg−Marquardt Algorithm. *J. Magn. Reson., Ser. A* **1996**, *120*, 155−189.
(31) Lazić, Z. R. *Design of Experiments in Chemical Engineering*; Wiley−VCH: Weinheim, 2004.
(32) Scheffe, H. Experiments with Mixtures. *J. R. Stat. Soc., B Met.* **1958**, *20*, 344−360.
(33) Scheffe, H. The Simplex-Centroid Design for Experiments with Mixtures. *J. R. Stat. Soc., B Met.* **1963**, *25*, 235−251.
(34) Cox, D. R. A Note on Polynomial Response Functions for Mixtures. *Biometrika* **1971**, *58*, 155−159.
(35) Benito-Peña, E.; Martins, S.; Orellana, G.; Moreno-Bondi, M. C. Water-Compatible Molecularly Imprinted Polymer for the Selective Recognition of Fluoroquinolone Antibiotics in Biological Samples. *Anal. Bioanal. Chem.* **2009**, *393*, 235−245.
(36) Goh, E. C. C.; Stöver, H. D. H. Cross-Linked Poly(methacrylic acid-*co*-poly(ethylene oxide) methyl ether methacrylate) Microspheres and Microgels Prepared by Precipitation Polymerization: A Morphology Study. *Macromolecules* **2002**, *35*, 9983−9989.
(37) Shim, S. E.; Yang, S.; Choi, H. H.; Choe, S. Fully Crosslinked Poly(styrene-*co*-divinylbenzene) Microspheres by Precipitation Polymerization and Their Superior Thermal Properties. *J. Polym. Sci., Part A: Polym. Chem.* **2004**, *42*, 835−845.
(38) Sundararajan, P. R. In *Physical Properties of Polymers Handbook*, 2nd ed; Mark, J. E., Ed.; Springer: New York, 2007; Chapter 15, pp 259−287.
(39) Li, W. H.; Stöver, H. D. H. Porous Monodisperse Poly(divinylbenzene) Microspheres by Precipitation Polymerization. *J. Polym. Sci., Part A: Polym. Chem.* **1998**, *36*, 1543−1551.
(40) *Molecularly Imprinted Polymers: Man-Made Mimics of antibodies and their Applications in Analytical Chemistry*; Sellergren, B., Ed.; Elsevier: Amsterdam, 2001.
(41) Yang, S.; Shim, S. E.; Lee, H.; Kim, G. P.; Choe, S. Size and Uniformity Variation of Poly(MMA-*co*-DVB) Particles upon Precipitation Polymerization. *Macromol. Res.* **2004**, *12*, 519−527.
(42) Shim, S. E.; Yang, S.; Choe, S. Mechanism of the Formation of Stable Microspheres by Precipitation Copolymerization of Styrene and Divinylbenzene. *J. Polym. Sci., Part A: Polym. Chem.* **2004**, *42*, 3967−3974.
(43) Manesiotis, P.; Borrelli, C.; Aureliano, C. S. A.; Svensson, C.; Sellergren, B. Water-Compatible Imprinted Polymers for Selective Depletion of Riboflavine from Beverages. *J. Mater. Chem.* **2009**, *19*, 6185−6193.
(44) Rampey, A. M.; Umpleby, R. J.; Rushton, G. T.; Iseman, J. C.; Shah, R. N.; Shimizu, K. D. Characterization of the Imprint Effect and the Influence of Imprinting Conditions on Affinity, Capacity, and Heterogeneity in Molecularly Imprinted Polymers Using the Freundlich Isotherm-Affinity Distribution Analysis. *Anal. Chem.* **2004**, *76*, 1123−1133.
(45) Rodriguez, E.; Navarro-Villoslada, F.; Benito-Peña, E.; Marazuela, M. D.; Moreno-Bondi, M. C. Multiresidue Determination of Ultratrace Levels of Fluoroquinolone Antimicrobials in Drinking and Aquaculture Water Samples by Automated Online Molecularly Imprinted Solid Phase Extraction and Liquid Chromatography. *Anal. Chem.* **2011**, *83*, 2046−2055.
(46) *CRC Handbook of Chemistry & Physics*, 90th ed; Lide, D. R., Ed.; CRC Press: Boca Raton, FL, 2010.
(47) Olsson, G. D.; Karlsson, B. C. G.; Shoravi, S.; Wiklander, J. G.; Nicholls, I. A. Mechanisms Underlying Molecularly Imprinted Polymer Molecular Memory and the Role of Crosslinker: Resolving Debate on the Nature of Template Recognition in Phenylalanine Anilide Imprinted Polymers. *J. Mol. Recognit.* **2012**, *25*, 69−73.

DOI: 10.1021/acsami.5b02238
ACS Appl. Mater. Interfaces 2015, 7, 10966−10976